

ON THE AIR-FLOW RESISTANCE OF TUNNEL FIRES IN LONGITUDINAL VENTILATION – THE “THROTTLING EFFECT”

¹Ingo Riess, ²Daniel Weber, ²Michael Steck,
¹Riess Ingenieur-GmbH, CH
²Amstein + Walthert Progress AG, CH

ABSTRACT

After having been reported in a series of articles in the late 1970s, the air-flow resistance of a tunnel fire in longitudinal ventilation (also known as “throttling effect”) has been investigated in several studies between 2006 and 2018, mostly by means of CFD calculations. These previous publications give different formulations for the “throttling effect”, mainly due to combining different factors in a single formulation.

In the present study, a detailed 1-D model of the various factors contributing to the air-flow resistance of a tunnel fire is described. For the description of these effects the static pressure is strictly considered. The following model characteristics are given:

- 1-D wall friction upstream of the fire
- Expansion and acceleration of the flow due to temperature rise
- 1-D wall friction downstream of the fire
- Compression and deceleration of the fire fumes due to cooling downstream of the fire
- Resistance due to temperature stratification downstream of the fire

The factors are studied using one-dimensional fluid dynamics (continuity, momentum balance, energy balance) except for the resistance due to temperature stratification. As this contribution is linked to wall friction and secondary flow in the stratified flow downstream of the fire, it is studied in more detail using numerical simulations.

Keywords: throttling effect, tunnel, fire, flow resistance, pressure drop, stratification, FireFoam

1. INTRODUCTION

Longitudinal tunnel ventilation systems are designed to provide a minimum airflow in the event of a fire. Usually, the design is based on a 1D steady-state model that is applied to several design scenarios. The methodology is described in design codes. In most of these models the assumption is made that the fire itself does not act as a flow resistance. Since the 1960s, it is known that a fire in a closed duct induces a pressure loss. But knowledge on this effect is rather limited and partly contradictory. There is a risk, that in tunnel ventilation design the “throttling effect” is underestimated and the ventilation systems are therefore insufficiently dimensioned.

We had the opportunity to study the “throttling effect” in an extensive research study funded by the Swiss Road Administration. This article includes the main findings. We expect the full report to be published in summer 2020.

2. PREVIOUS WORK

For the purpose of this article we restrict the description of previous work on four publications. All of them include a formulated approach on how the “throttling effect” is calculated:

F_R describes the wall friction force in the three sections and Q the heat release rate. We neglect the fuel mass flux \dot{m} . It has only a small impact and is omitted here for readability of the equations. The local friction at the fire site F_{R2} can be treated with the friction in the adjacent section. The length L_2 is taken as 0.

The static pressure variation Δp in the entry section ①→② is calculated from the friction factor λ as

$$\Delta p_{0-1} = -\frac{\rho_0}{2} \cdot u_0^2 \cdot \frac{\lambda \cdot L_1}{D_h} \quad (1)$$

The static pressure variation through the fire ②→③ is calculated from the momentum balance as

$$\Delta p_{1-2} = -\frac{Q_c u_0}{c_p A_T T_0} \quad (2)$$

The static pressure variation in the third section ③→④ consists of three contributions:

- Wall friction as in section 1 but increased due to the expansion of the heated air and therefore increased flow velocity $u > u_0$

$$\Delta p_{2-3A} = -\frac{\lambda \rho_0}{2 D_h} u_0^2 \cdot \left[\frac{Q_c}{\alpha U_T T_0} \left(1 - \exp \left(-\frac{\alpha U_T L_3}{\rho_0 u_0 A_T c_p} \right) \right) + L_3 \right] \quad (3)$$

The circumference of the tunnel profile is given as U_T , the heat transfer coefficient to the tunnel wall as α .

- The regained static pressure due to cooling of the smoke and therefore reduced flow velocity $u < u_2$

$$\Delta p_{2-3B} = \frac{Q_c u_0}{c_p A_T T_0} \left(1 - \exp \left(-\frac{\alpha U_T L_3}{\rho_0 u_0 A_T c_p} \right) \right) \quad (4)$$

- The additional static pressure drop due to temperature stratification (additional friction and energy dissipation in the secondary flow)

$$\Delta p_{2-3C} = -1.894 \frac{Q^{0.315} u_0^{1.136} H_T^{0.608}}{A_T^{1.295}} \cdot \frac{L_3}{500 \text{ m}} \quad (5)$$

H_T represents the height of the tunnel profile. Q , u_0 , H_T , A_T and L_3 are applied in standard units [W], [m/s], [m], [m²] and [m]. Eq. (5) is derived from the 3D CFD simulations described in section 4 of this article.

The sum of equations (1) to (5) leads to the static pressure difference ①→④. In order to separate the “throttling effect” of the fire, the cold flow wall friction must be subtracted.

$$\Delta p_{throttling} = \Delta p_{0-1} + \Delta p_{1-2} + \Delta p_{2-3A} + \Delta p_{2-3B} + \Delta p_{2-3C} - \left(-\frac{\rho_0}{2} \cdot u_0^2 \cdot \frac{\lambda \cdot (L_1 + L_3)}{D_h} \right) \quad (6)$$

4. SIMULATION

4.1. CFD model

Initially, the intention was to use the Fire Dynamic Simulator for the evaluation of the “throttling effect”. After a series of test cases, frequent discussions with fellow users in the online forum and some correspondence with the authors of FDS, it was concluded that FDS in its current form (versions 6.5.2 to 6.7.3) is not capable to reliably model the pressure field near a fire in a long stretched computational domain. Other authors came to a similar conclusion (Pachera, Deckers, & Beji, 2018).

Consequently, further modelling has been based on FireFoam, an application within the standard distribution of OpenFOAM. For our study we considered FireFoam an engineering tool: The underlying equations and sub-models of FireFoam are described in the documentation and not detailed here. The influence of various model parameters and sub-models was evaluated in the initial phase of the project. It was found that the default parameters were appropriate.

For the computational domain a structured mesh approach was selected. The tunnel geometry was varied from a two-lane rectangular profile to a four-lane horse-shoe profile and the length of the computational domain extended from 100 m upstream to 500 m downstream of the fire. For a few simulations the domain was extended 1000 m downstream of the fire. The maximum width of the grid cells is 33 cm with the resolution being increased towards the tunnel walls and ceiling. A grid sensitivity study was performed leading to the conclusion that a further reduction of grid size would not change the pressure field significantly. For such an extensive parameter variation, the grid size is always a compromise between computation time and accuracy.

To model the fire, a section of external cell faces is selected where a continuous stream of methane enters the domain. The methane mixes with the tunnel air and reacts spontaneously with oxygen. For this reaction the Eddy Dissipation Model is used. A model for heat radiation is included in the simulation. The heat release rate was varied between 2 MW and 34 MW. Larger fires were difficult to simulate, as thermo-acoustic oscillations were observed with a coupled oscillation of heat release rate, pressure and flow velocity (thermo-acoustic instability, Rijke tube). A more detailed description of this phenomenon will be part of the project report.

Flow turbulence is modelled using a compressible Large Eddy Simulation with an underlying k-equation sub-model. The calculation includes a hydrostatic pressure field. However, for the evaluation of the static pressure in the tunnel, the pressure p_{rgh} is selected. This represents the static pressure without the hydrostatic pressure field (i.e. the “gauge pressure”).

At the entry portal the flow is described by a typical turbulent flow profile. This is not precisely the fully developed flow profile in a tunnel, but it allows the pressure profile along the tunnel to show the expected linear behavior after a length of approx. $5 D_h$. At the exit portal the static pressure is given as ambient pressure ($p_{rgh} = 0$). For the tunnel walls and ceiling a friction factor corresponding to a surface roughness of 2.5 mm is applied.

For the temperature boundary condition of the tunnel walls, FireFoam allows the definition of a mixed boundary. A comparison was made between the calculated temperature curve along the domain and the temperature curve given in the Austrian RVS 09.02.31. It was found that a mixture of 97% adiabatic and 3% isothermal temperature boundary condition coincides with the RVS.

4.2. Qualitative description of the flow field

In this section, the flow field of a typical simulation (2-lane tunnel, horse-shoe profile, 8 MW fire, inflow 3 m/s) is described in some detail. As there is only very limited experimental data available, the flow field is described and evaluated against known flow phenomena. Due to space limitations this description must remain incomplete here. A more detailed description will be given in the project report.

In the 100 m long entry section the flow profile is governed by the inlet boundary condition. The distance is insufficient to develop the regular turbulent tunnel flow. The static pressure profile shows the expected linear behavior after approx. $5 D_h$.

At the methane inlet (“burner”) the fuel is diluted rapidly. The energy conversion occurs mostly along the rim of the burner. The initial dilution of the fire fumes CO_2 and H_2O also occurs rapidly. The flow field of the fire plume shows periodic fluctuations according to the characteristic frequency of a diffusion flame from an area source. **Figure 2** shows instantaneous

(no time-average) streamlines originating from the burner. The two rotating cells of the secondary flow are visible. The secondary flow is caused by the buoyant plume being deflected in the longitudinal airflow. This phenomenon is well described in the literature.

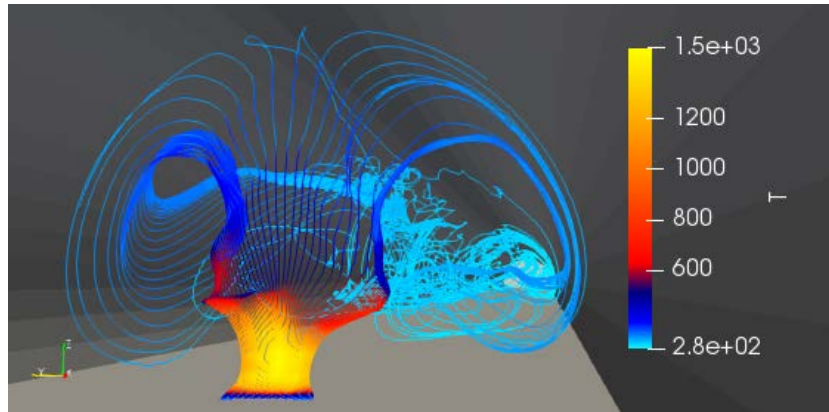


Figure 2: Streamlines originating from the methane inlet

Further downstream, a different type of secondary flow is developed, as shown in **Figure 3**. This flow pattern looks rather similar, consisting of two cells as well. But this flow is driven by cooling of the fire fumes at the tunnel ceiling. The hot flow is rising towards the ceiling, cooled and moved sideways along the tunnel profile where the cool air moves downward. The temperature reduction can be read from the color code used for the streamlines. This secondary flow stabilizes the temperature stratification downstream of the fire. It is much weaker than the one shown in **Figure 2**, moving the cells little more than a full circle over a 500 m distance.

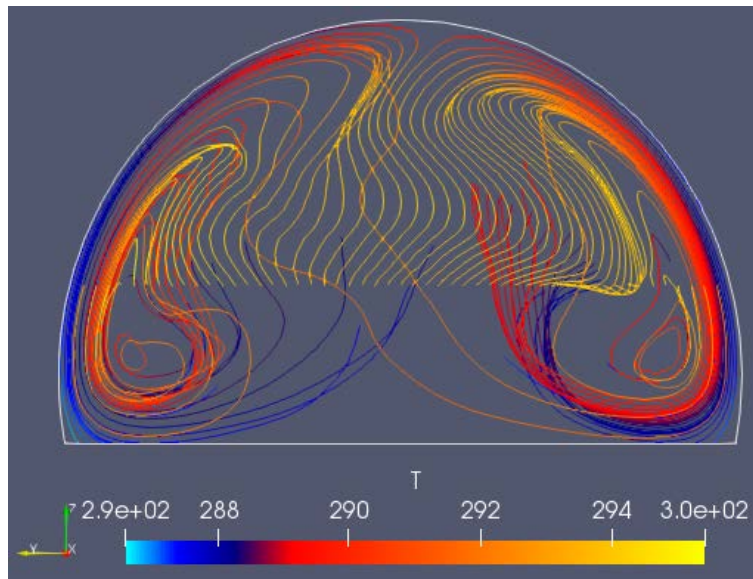


Figure 3: Streamlines between 500 m and 1000 m downstream of the fire

Figure 4 shows flow profiles for different sections of the tunnel. The flow profiles are instantaneous, i.e. without application of a time average. Upstream of the fire the flow profile is determined by the profile applied as inlet boundary condition. At the fire site the flow profile is completely disrupted due to the periodic fluctuations of the plume, the buoyancy of the fire gases and the secondary flow induced by the plume in crossflow.

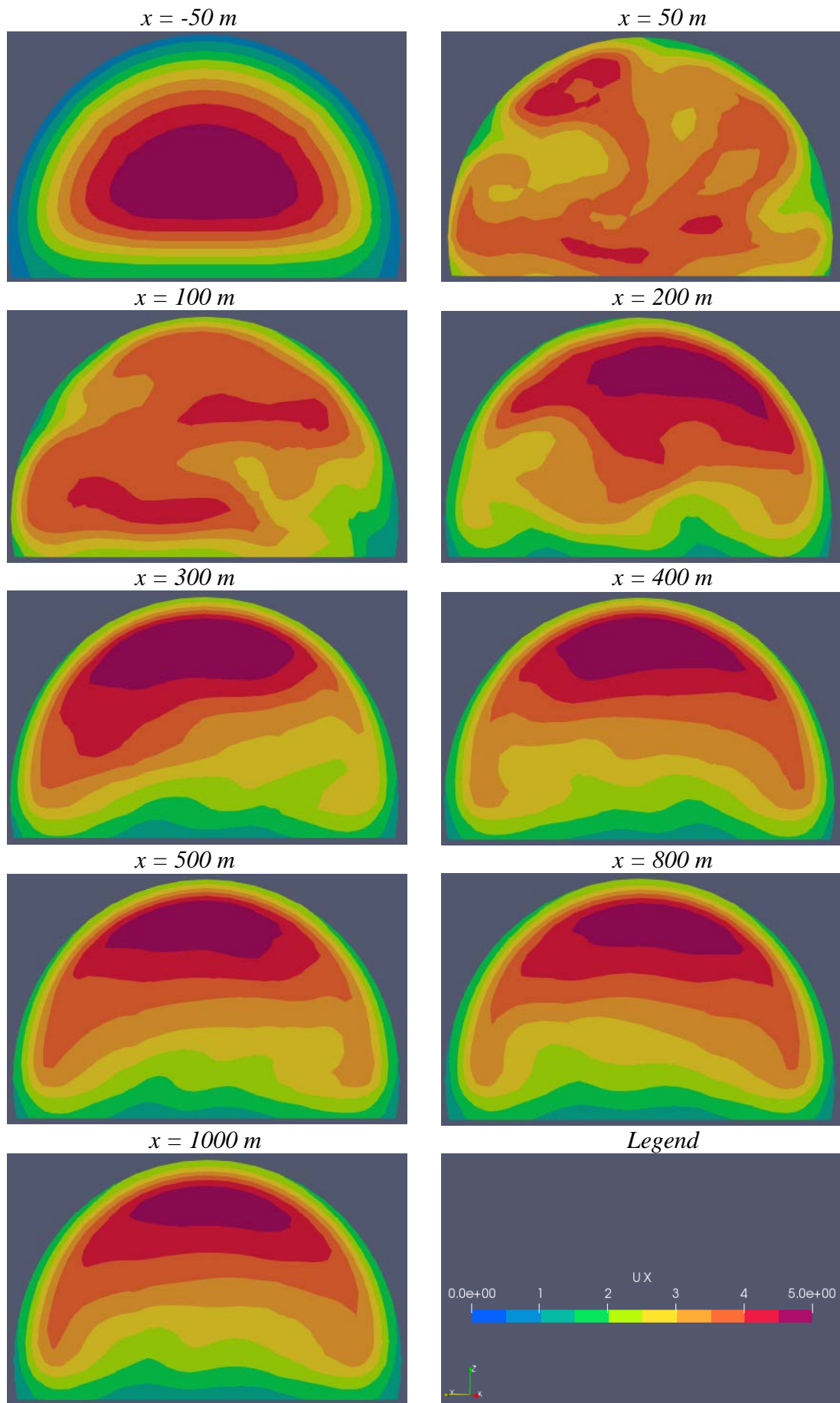


Figure 4: Flow profile for various tunnel sections [m/s]

However, about 200 m downstream of the fire the flow field begins to reorganize into a stratified flow profile with the maximum airflow velocity close to the tunnel ceiling. The flow profile develops into a mushroom shape with slightly higher flow velocity at the tunnel wall. This corresponds very well to the secondary flow shown in **Figure 3**.

It is further visible that the flow pattern does not evolve back into the expected turbulent flow profile that was present upstream of the fire. Instead, the maximum flow velocity remains close to the tunnel ceiling even 1000 m downstream from the fire – which in this case represents $125 D_h$. The reason for the stability of this stratified flow is visualized in the corresponding temperature distribution, see **Figure 5**. The color code has been selected in order to demonstrate the similarity between the airflow and temperature profile. Although the absolute temperature variation in the cross-section is reduced to only 4 K, the profiles of temperature and airflow velocity are practically identical. In this article we refer to stratification as temperature or density stratification only. This must not be mixed-up with smoke stratification.

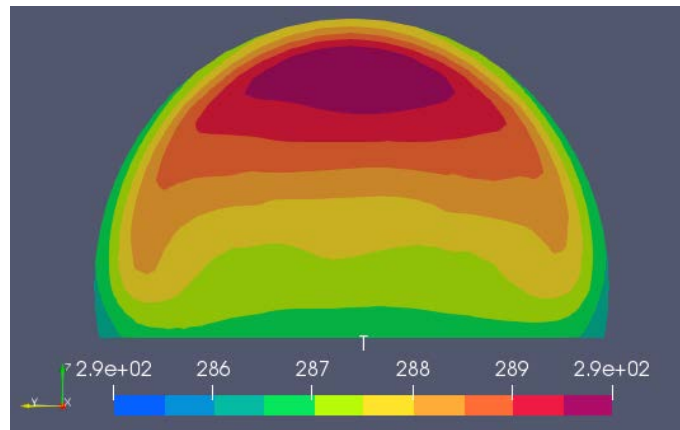


Figure 5: Temperature profile [K] at $x = 1000$ m

As a general principle, this temperature distribution can be interpreted as an application of the Reynolds analogy. The Reynolds analogy provides a relation between turbulent momentum and heat transfer. In turbulent flow, momentum and heat transport depend on the same turbulent eddies. Therefore, velocity and temperature profiles have the same shape. The analogy is valid if the turbulent Prandtl number is close to unity and in the absence of flow separation or form drag. Both conditions are met in this simulation.

Figure 6 shows the static pressure variation along the extended computational domain. The red line shows the local data for locations at 10 m intervals along the tunnel. The dashed line gives an idealized profile assuming a linear curve both upstream and downstream of the fire with a local pressure reduction at the fire.

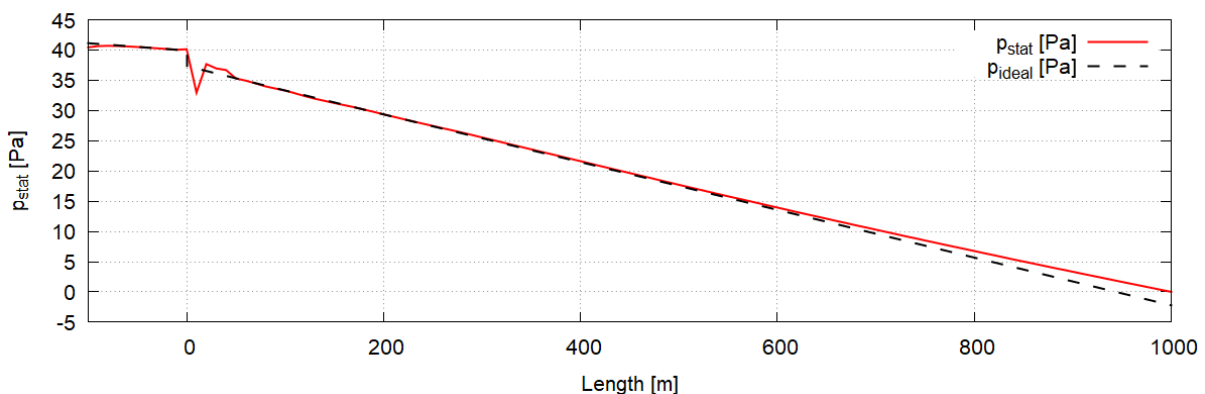


Figure 6: Static pressure along the tunnel, 8 MW fire at 0 m

The pressure profile shows the linear pressure reduction upstream of the fire that is consistent with equation (1). A small deviation is visible directly at the entry boundary condition. Near the fire the pressure fluctuates due to local airflow velocity close to the fire plume. About 50 m downstream of the fire the pressure profile shows a nearly linear pressure reduction that remains at a constant gradient until being reduced gradually from about $x = 500$ m onward. Still, even 1000 m downstream the local pressure reduction is increased significantly when compared to the cold flow approaching the fire. This corresponds to the airflow profile shown in **Figure 4**.

4.3. Results

In an initial test series, various parameters were excluded as not having a significant impact on the “throttling effect”. It was found that the wall friction coefficient, the shape of the fire source and the location of the fire along the width of the tunnel do not have a significant impact on the pressure resistance.

We also investigated the height of the fire source in the tunnel profile. While this has a significant impact on the pressure drop, it was omitted from our parameter variation. The flow downstream of the fire was affected qualitatively, what made a numerical fit such as equation (7) questionable. Furthermore, a fire at road level can be assumed as the worst-case scenario. Elevated fires showed a smaller pressure resistance.

We further investigated the presence of vehicles in the vicinity of the fire, yet the results were non-conclusive (minor impact of vehicles on the pressure resistance) and the number of possible different fire scenarios proved prohibitive for a parameter study.

In accordance with previous work on the “throttling effect” the main parameters were defined as

- heat release rate Q (varied from 2 MW to 34 MW),
- upstream airflow velocity u_0 (varied from 1 m/s to 4 m/s),
- tunnel cross-section A_T (varied from 52 m² to 136 m²), and
- height of the tunnel profile H_T (varied from 5.2 m to 9 m).

The tunnel cross-section was selected against the hydraulic diameter D_h as a more consistent data fit was achieved using the tunnel cross-section. The height of the tunnel profile was included as this allowed a better data fit, especially when the four-lane tunnel profiles (horse-shoe and rectangular) were evaluated. In the parameter variation L_3 was selected as 500 m.

The static pressure difference ①→③ is read from the linearized pressure profile. In the next step the static pressure difference is corrected by subtracting the pressure drop contributions in equations (1) to (4). This is done for each simulation. The remaining contribution from the stratified flow is then calculated from

$$\Delta p_{throttling} = A \cdot Q^B \cdot u_0^C \cdot A_T^D \cdot H_T^E \quad (7)$$

With the proportional constant A and the exponents B , C , D and E being determined from a function fit to the data derived from all simulations. The data set had to be cleaned-up as some pressure profiles could not be used due to excessive periodic pressure fluctuations or due to smoke back-layering reaching the inflow boundary condition for scenarios with an inflow velocity of 1 m/s. The fit function was evaluated using the fitting routine that is included in the software package Gnuplot V5.2. The results for parameters A to E are shown in **Table 2**.

Table 2: Final set of parameters

Final set of parameters	Asymptotic Standard Error
A = 1.89399	±0.2985 (15.76%)
B = 0.314672	±0.009252 (3.597%)
C = 1.13617	±0.04087 (2.94%)
D = -1.29471	±0.05016 (3.874%)
E = 0.608199	±0.06544 (10.76%)

It is stated that equation (7) is valid only for the 500 m long tunnel section downstream of the fire. Given the nearly linear effect of the stratified flow shown in **Figure 6**, the throttling effect extends beyond that point. Therefore, we extend equation (7) to

$$\Delta p_{throttling} = A \cdot Q^B \cdot u_0^C \cdot A_T^D \cdot H_T^E \cdot \frac{L_3}{500m} \quad (8)$$

In all scenarios the temperature stratification remained stable for a minimum of 500 m downstream of the fire. In a real fire situation, additional flow disturbances might limit the extent of the stratified flow conditions. We must leave it to the ventilation designer to estimate the extent of the temperature stratification beyond the 500 m modelled in our simulations.

A graphical representation of the data fit for all scenarios is given in **Figure 7**. The vertical axis is marked as a function of the heat release rate as this number does not have any physical meaning. The graph shall only demonstrate the quality of the fit, respectively the scatter of the data points.

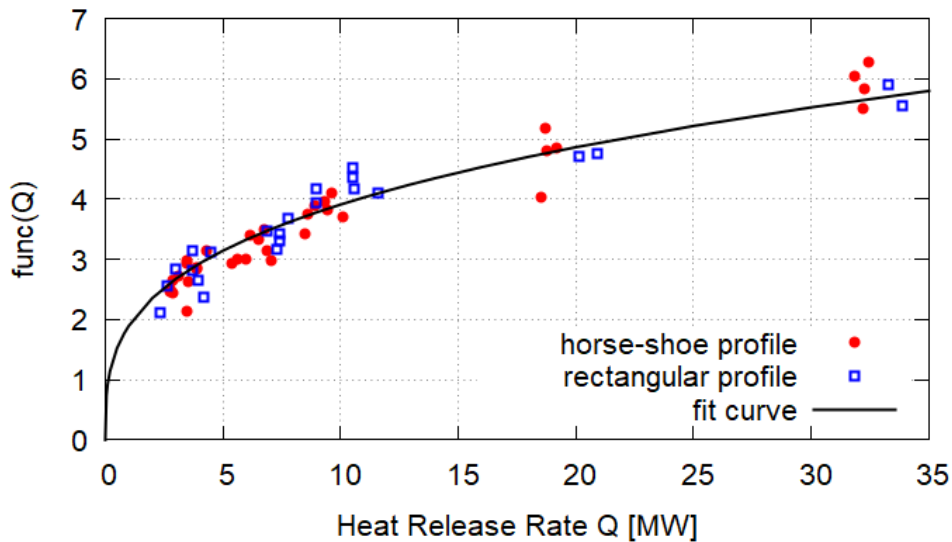


Figure 7: Simulation data and fitted curve

Figure 8 gives a comparison of the static pressure along the tunnel for a 32 MW fire in a 2-lane horse-shoe tunnel profile with a longitudinal flow of 3 m/s. The red line marks the results of the CFD simulation. The orange dotted line marks the linearized profile as read from the simulation data. The dashed blue line marks the results of the model as described by equations (1) to (6).

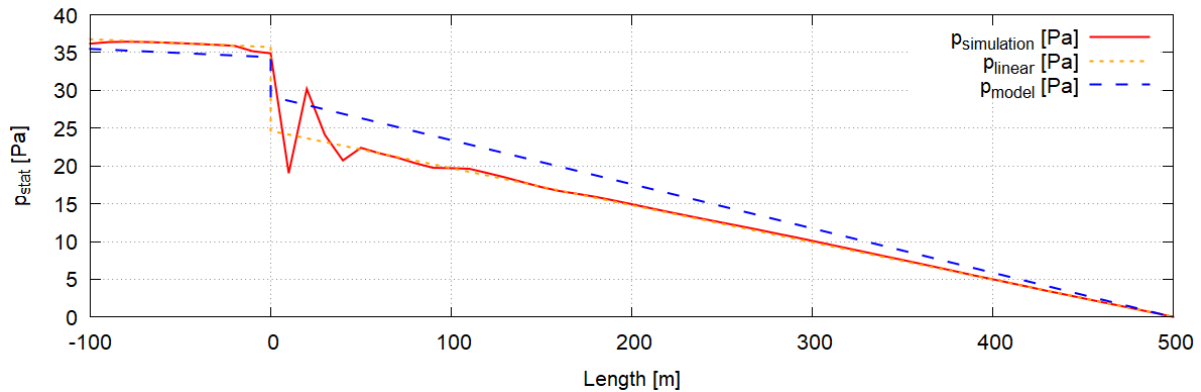


Figure 8: Static pressure along the tunnel, 32 MW fire at 0 m

5. CONCLUSION

This study confirms the observation of a pressure drop due to a tunnel fire in longitudinal ventilation. The “throttling effect” is described as the sum of several contributions, i.e.

- expansion and acceleration due to temperature rise at the fire,
- increased wall-friction downstream of the fire due to increased airflow velocity of the expanded tunnel air,
- compression and deceleration of the fire fumes due to cooling downstream of the fire, and
- flow resistance due to temperature stratification downstream of the fire.

It was found that the temperature stratification downstream of the fire contributes to the pressure drop even far beyond the extent of the fire. The model described in this paper allows an assessment of the “throttling effect” in one-dimensional simulation tools. The aerodynamic resistance of fires in road tunnels are relevant for the design and operation of longitudinal ventilation systems. The additional pressure resistance of a 30 MW fire in a 2-lane tunnel with a longitudinal flow of 3 m/s is estimated as 30 Pa along a 500 m distance downstream of the fire. Such a pressure drop may require the installation of additional groups of jet fans.

It must be noted that further research is required in order to assess the extent of a thermally stratified flow downstream of a tunnel fire. And the CFD simulations shown in this paper should be supported by further experimental evidence.

6. REFERENCES

- Centre d'Etudes des Tunnels. (2003). *Les dossiers pilotes du CETU - Section 4.1 Ventilation*.
- Du, T., Yang, D., & Ding, Y. (2018). Driving force to prevent smoke backlayering in downhill tunnel fires using forced longitudinal ventilation. *Tunneling and Underground Space Technology* 79, 76-82.
- Dutrieue, R., & Jacques, E. (2006). Pressure loss caused by fire in a tunnel. *12. Int. Symp. Aerodynamics and Ventilation of Vehicle Tunnels*. Portoroz.
- Fleming, C., Clark, G., Meeks, K., & Wicht, T. (2016). The treatment of the throttling effect in incompressible 1-D solvers. *8. Int. Conf. Tunnel Safety and Ventilation*. Graz.
- Pachera, M., Deckers, X., & Beji, T. (2018). Capabilities and limitations of the fire dynamic simulator in the simulation of tunnel fires with a multi-scale approach. *Journal of Physics, Conference Series* 1107 042016.